Early appearance of dendritic alterations in neocortical pyramidal neurons of the Ts65Dn model of Down syndrome

Early Appearance of Dendritic Alterations in Neocortical Pyramidal Neurons of the Ts65Dn Model of Down Syndrome

Beatrice Uguagliati[a] Fiorenza Stagni[b] Marco Emili[a] Andrea Giacomini[a]
Carla Russo[b] Sandra Guidi[a] Renata Bartesaghi[a]

[a]Department of Biomedical and Neuromotor Sciences, University of Bologna, Bologna, Italy;
[b]Department for Life Quality Studies, University of Bologna, Bologna, Italy

Keywords
Down syndrome · Ts65Dn model · Developing brain: dendritic development · Dendritic pathology · Pyramidal neurons · Frontal cortex

Abstract
Down syndrome (DS), which is due to triplication of chromosome 21, is constantly associated with intellectual disability (ID). ID can be ascribed to both neurogenesis impairment and dendritic pathology. These defects are replicated in the Ts65Dn mouse, a widely used model of DS. While neurogenesis impairment in DS is a fetal event, dendritic pathology occurs after the first postnatal months. Neurogenesis alterations across the life span have been extensively studied in the Ts65Dn mouse. In contrast, there is scarce information regarding dendritic alterations at early life stages in this and other models, although there is evidence for dendritic alterations in adult mouse models. Thus, the goal of the current study was to establish whether dendritic alterations are already present in the neonatal period in Ts65Dn mice. In Golgi-stained brains, we quantified the dendritic arbors of layer II/III pyramidal neurons in the frontal cortex of Ts65Dn mice aged 2 (P2) and 8 (P8) days and their euploid littermates. In P2 Ts65Dn mice, we found a moderate hypotrophy of the apical and collateral dendrites but a patent hypotrophy of the basal dendrites. In P8 Ts65Dn mice, the distal most apical branches were missing or reduced in number, but there were no alterations in the collateral and basal dendrites. No genotype effects were detected on either somatic or dendritic spine density. This study shows dendritic branching defects that mainly involve the basal domain in P2 Ts65Dn mice and the apical but not the other domains in P8 Ts65Dn mice. This suggests that dendritic defects may be related to dendritic compartment and age. The lack of a severe dendritic pathology in Ts65Dn pups is reminiscent of the delayed appearance of patent dendritic alterations in newborns with DS. This similarly highlights the usefulness of the Ts65Dn model for the study of the mechanisms underlying dendritic alterations in DS and the design of possible therapeutic interventions.

Introduction

Dendritic pathology appears to be a consistent feature in genetic intellectual disabilities (IDs) [1–5] and is one of the typical phenotypic features of Down syndrome (DS). DS, which is due to triplication of chromosome 21, is the most common genetic condition associated with ID. Brain size is reduced in infants and fetuses with DS due to a widespread reduction in the process of neurogenesis and, consequently, hypocellularity in numerous brain regions (see [6]). Moreover, individuals with DS are characterized by a dendritic pathology that involves both dendritic length and spine density (see [7]). A reduction in spine density and dendritic hypotrophy has been found in neocortical and hippocampal neurons of adults with DS; these defects are worsened by neurodegeneration at later life stages caused by the occurrence of Alzheimer disease [8–11]. Unlike neurogenesis impairment, dendritic pathology is no present at fetal and very early neonatal stages. A large study by Takashima et al. [12] examined neurons of the visual cortex of fetuses, neonates, and adults with DS; spine dysgenesis was not detected in fetuses with DS but was present at later ages. That study also evaluated the dendritic length in the visual cortex of fetuses and infants with DS and found a reduction in the length of the basal dendrites in infants with DS who were older than 4 months. Becker et al. [13] evaluated the dendritic branching and length of apical and basal dendrites in the visual cortex. They found that in infants younger than 6 months, both parameters were larger than in controls but that they started to be reduced after 2 years of age. A subsequent study by Prinz et al. [14] showed that a 3-month-old infant with DS had cortical

interneurons with lower dendritic areas and a higher number of branching points. Schulz and Scholz [15] evaluated the pyramidal neurons in 2 children (20 months of age or 6 years of age) with DS and found that the neurons of the older child exhibited larger abnormalities. Vuksic et al. [16] examined the dendritic arbor of prefrontal-cortex layer III pyramidal neurons in an infant with DS aged 2.5 months and found no differences in comparison with an age matched control. This evidence suggests that unlike neurogenesis impairment, which is a fetal event, dendritic pathology is a slightly later event that occurs in infancy. Dendritic alterations in the infantile period, a critical period for synapse formation, crucially impact on the final brain wiring. Thus, early dendritic pathology, in conjunction with neurogenesis alterations, must be regarded as a key determinant of the ID that characterizes DS.

Mouse models are fundamental for identification of the pathogenetic mechanisms in DS and the design of therapeutic interventions. Various mouse models of DS have been created carrying triplication of different sets of genes homologous to those of HSA21 [17]. The Ts65Dn mouse is the best characterized and the more widely used model of DS because it replicates numerous phenotypicfeatures of DS, including, reduction of neurogenesis, dendritic pathology, and cognitive impairment [18]. Studies in adult Ts65Dn mice showed severe proliferation impairment in the subgranular zone of the hippocampus and subventricular zone of the lateral ventricle (see [7]), the two major neurogenic niches of the forebrain, that keep a neurogenic potential in adulthood. There is additionally evidence that Ts65Dn mice already exhibit neurogenesis impairment in the preand early postnatal period (see [6]). Thus, the developmental phenotype of the Ts65Dn mouse appears to parallel the human condition as far as neurogenesis is concerned. The very few studies that focused on the dendritic pattern in Ts65Dn mice were conducted at adult life stages. Those studies showed reduced density of dendritic spines and dendritic hypotrophy in hippocampal [19–22] and neocortical [2] neurons. Regarding the onset of these defects, a single recent study shows that Ts65Dn mice aged 8 days already exhibit defects in the dendritic arborization of hippocampal granule neurons [23], indicating early impairment in hippocampal dendritic development in this model of DS. It is not known, however, whether neocortical neurons of Ts65Dn mice exhibit, similarly to infants with DS, early dendritic alterations. In order to fill this gap, in the current study, we have examined the dendritic arbor of pyramidal neurons in the frontal neocortex of Ts65Dn pups aged 2 and 8 days. We selected this cortical region because it is involved in higher order cognitive functions, including nonspatial memory [24], that are impaired in children (and adults) with DS [25].

Methods

Colony

Ts65Dn mice were generated by mating B6EiC3Sn a/A-Ts(17^{16})65Dn females (JAX line 1924; Ts65Dn females) with C57BL/6JEiJ × C3H/HeSnJ (B6EiC3Sn) first generation (F1) hybrid males (JAX line 1875; euploid males). This parental generation was provided by Jackson Laboratories (Bar Harbor, ME, USA). Our colony typically includes 10–12 Ts65Dn females and 10–12 euploid males provided by the Jackson Laboratories and used as breeders for the duration of their effective reproductive cycles (5–6 cycles). The colony is then renewed with new breeders provided by the Jackson Laboratories. In order to maintain the original genetic background, we use for our studies mice of the F1 or, occasionally, of the second generation. The latter is obtained by crossing F1 Ts65Dn females with euploid males provided by the Jackson Laboratory. The mice used here were mice of the first generation. Animals were genotyped as previously described [26]. The day of birth was designated as postnatal day 0. The animals' health and comfort were controlled by the veterinary service. The animals had access to water and food ad libitum and lived in a room with a 12:12 h light/dark cycle. Experiments were performed in accordance with the European Communities Council Directive of 24 November 1986 (86/609/EEC) for the use of experimental animals and were approved by Italian Ministry of Public Health. In this study, all efforts were made to minimize animal suffering and to keep the number of animals used to a minimum.

Experimental Protocol

The progeny obtained by breeding Ts65Dn females (n = 8) with euploid males (n = 8) was euthanized either on postnatal day 2 (P2; 4 litters) or on postnatal day 8 (P8; 4 litters). The brains were excised, cut along the midline, and put in a Golgi solution (see below). Analyses were carried out on the brains of P2 Ts65Dn (n = 7; sex = 5 males and 2 females) and euploid (n = 7; sex = 5 males and 2 females) littermates and P8 Ts65Dn (n = 7; sex = 5 males and 2 females) and euploid (n = 5; sex = 5 males) littermates. Ts65Dn pups derived from all litters entered the study.

Histological Procedures

Golgi Staining

Brains were Golgi-stained using the FD Rapid GolgiStain™ Kit (FD NeuroTechnologies, Inc.). Brains were immersed in the impregnation solution containing mercuric chloride, potassium dichromate, and potassium chromate (the impregnation solution was prepared by mixing equal volumes of Solutions A and B of the FD Rapid GolgiStain™ Kit) and stored at room temperature in the dark for

2 weeks. Then, brains were transferred into Solution C (FD Rapid GolgiStain™ Kit) and stored at room temperature in the dark for at least 72 h. After these steps, hemispheres were cut with a microtome into 90-μm-thick coronal sections that were mounted on gelatin-coated slides and were air-dried at room temperature in the dark for at least 1 day. After drying, sections were rinsed with distilled water and subsequently stained in a developing solution (FD Rapid GolgiStain Kit).

Measurements

Neuron Sampling

Measurements were carried out in neurons from the right hemisphere, for consistency with our previous analysis of hippocampal granule neurons [23]. The Golgi method casually impregnates a few neurons among a given population and allows one to sample relatively isolated neurons. Golgi-stained neurons were sampled from layer II/III of the frontal neocortex in sections comprised between the stereotaxic planes 1.23–2.43 [27] (Fig. 1a, d). The total number of sampled Golgi-stained neurons was 7–9 per animal. Only well-impregnated neurons were chosen for the histological analysis. The drawings were made on coded slides so that the drawer was not aware of the animal's genotype.

Measurement of the Dendritic Trees and Soma

The following system was used: (i) light microscope (Leitz) equipped with a motorized stage and focus control system; (ii) color digital video camera attached to the microscope; (iii) Image-Pro Plus (Media Cybernetics, Silver Spring, MD, USA) with the StagePro module for controlling the motorized stage in the *x*, *y*, and *z* directions, as primary software. Apical and basal dendritic trees of Golgi-stained neurons were traced with a software custom-designed for dendritic reconstruction (Immagini Computer, Milan, Italy), interfaced with Image-Pro Plus. The apical and basal dendritic trees were traced live, at a final magnification of ×500, by focusing into the depth of the section. The operator starts with two branches emerging from the cell soma and after having drawn the first parent branch goes on with all daughter branches of the next order in a centrifugal direction (Fig. 1e). At the end of tracing, the program reconstructs the number and length of individual branches, the mean length of branches of each order, and total dendritic length. We additionally evaluated the number of dendritic segments that emerged from the main apical dendritic shaft (collateral dendrites; Fig. 1e). Measurements of the surface area and major axes of the soma were carried out with the software Image-Pro Plus at a final magnification of ×500.

Measurement of Spine Density

Spines on the soma and basal dendrites of pyramidal neurons of layer II/III were counted live using a ×100 oil immersion objective lens (Leitz microscope and objective with 1.4 NA). In P2 mice, somatic spines were counted along the whole soma circumference.

The thickness of the dendritic processes emerging from the soma was evaluated and subtracted from the total soma circumference in order to obtain the "effective soma circumference." The linear spine density was calculated by dividing the total number of counted spines by the soma effective circumference. Spine density was expressed as the number of spines per 10 μm somatic length. In P8 mice, basal dendritic spines were evaluated in firstand secondorder basal dendritic segments (n = 3–8 segments per neurons). For each animal, spines were counted in 6–9 neurons, for a total of 27–45 segments per animal. The length of each sampled dendritic segment was determined by tracing its profile, and the number of spines was counted manually. The linear spine density was calculated by dividing the total number of spines by the length of the dendritic segment. Spine density was expressed as the number of spines per 10 μm dendrite.

Statistical Analysis

Results are presented as mean ± SEM. Data were analyzed with the IBM SPSS 22.0 software. Before running statistical analyses, we checked data distribution and homogeneity of variances for each variable using the Shapiro-Wilk test and Levene's test, respectively. Statistical analysis was based on a priori planned comparisons [28]; we compared P2 Ts65Dn mice to P2 euploid mice and P8 Ts65Dn mice to P8 euploid mice. If the data were normally distributed and variance was homogeneous, statistical analysis was carried out using the two-tailed Student's t test. If the data were not normally distributed and variance was heterogeneous, transformations were made to achieve normality. If the transformed data did not achieve normality, statistical analysis was carried out using the Mann-Whitney U test. Based on the "Box plot" tool available in SPSS Descriptive Statistics, in each analysis, we excluded the extremes, i.e., values that were larger than 3 times the IQ range [$x \geq$ Q3 + 3 × (IQ); $x \leq$ Q1 − 3 × (IQ)]. A probability level of $p \leq 0.05$ was considered to be statistically significant.

Results

Pattern of the Neurons in Layer II/III of the Frontal Cortex of P2 and P8 Mice: Qualitative Observations In the current study, we sampled neurons from the superficial layers of the frontal cortex because deep-layer neurons were scarcely impregnated in Golgi-stained material of P2 and P8 euploid and Ts65Dn mice. While layer I was clearly recognizable, it was not possible to distinguish layer II from layer III. Therefore, we will call layer II/III the region where neurons of the current study were sampled.

Golgi-stained neurons in layer II/III of P2 and P8 euploid and Ts65Dn mice had an elongated soma, an apical dendritic tree, and basal dendrites (Fig. 1c, e, 2a, b, 3). The shaft of the apical dendrite emerged from the top of the

soma and extended toward layer I, irrespective to the depth of the soma within layer II/III (Fig. 2a). The apical shaft emitted collateral dendrites (Fig. 1c–e) that could give origin to secondary and, more rarely, to tertiary branches. We will call here "apical dendrites" the main apical trunk plus its distal tuft. Although collateral dendrites belong to the apical dendritic domain, they will be considered here separately and referred to as "collateral dendrites" (Fig. 1e). Basal dendrites were emitted from the base as well as from the circumference of the soma. In P2 euploid and Ts65Dn mice, very few neurons (<5% of the sampled neurons) had an immature shape (Fig. 2c), as indicated by their ovoid cell body; the presence of numerous varicosities along the stem apical dendrite(Fig. 2c, arrowheads); and the scarce number of apical, collateral, and basal dendritic branches. The pyramidal neurons of P8 euploid and Ts65Dn mice had a more mature pattern in comparison with those of P2 mice because both their apical and basal dendrites branched more profusely and were spatially more expanded, and their soma had a larger size (Fig. 3). In some neurons of P2 and P8 euploid and Ts65Dn mice, an axon emerging from the base of the soma and directed to the deep layers could be detected (Fig. 2a, 3b–d: empty arrow).

Apical, collateral, and basal dendrites of P2 euploid and Ts65Dn mice lacked dendritic spines (Fig. 2d, e), which is consistent with the generation of dendritic spine approximately at the end of the first postnatal week in rodents [29–32]. Protrusions with the appearance of stubby spines, however, were present on the soma (Fig. 2d, e: arrows). This is in agreement with the early appearance of somatic spines in the period P1-P5 in rodents [29, 30, 33, 34]. Occasionally, spines were detected on the portion of the primary apical dendrite close to its emergence from the soma (Fig. 2d, e: white arrowhead). In P8 euploid and Ts65Dn mice, somatic spines were less clearly detectable. In contrast, spines were present on both apical and basal (Fig. 2f) dendritic branches.

Pattern of Pyramidal Neurons in P2 and P8 Ts65Dn and Euploid Mice: Qualitative Observations

Figure 3 shows examples of pyramidal neurons in Ts65Dn and euploid mice aged 2 and 8 days. Ts65Dn mice aged 2 days had pyramidal neurons with apical and basal dendritic trees more scarcely ramified in comparison with euploid mice. This difference was more readily detectable regarding the basal dendrites (Fig. 3a, b). In contrast, in Ts65Dn mice aged 8 days, no patent differences in the basal and apical dendritic arborization were detectable in comparison with their euploid counterparts (Fig. 3c, d). At both ages, the soma of the pyramidal neurons of euploid mice had a large width and a pyramidal shape (Fig. 3a, c); in contrast, in Ts65Dn mice, the soma had a narrower width and a more ovoid shape (Fig. 3b, d).

Quantification of the Apical Dendrites of Pyramidal Neurons in P2 and P8 Euploid and Ts65Dn Mice

An evaluation of the total length, number of branches, and mean branch length of the apical dendritic tree showed no difference between euploid and Ts65Dn mice both at P2 (Fig. 4a–c) and P8 (Fig. 4g–i). In order to analyze dendritic morphology in detail, we examined each dendritic order separately. As expected, there was an age related increase in the maximum number of dendritic orders that from a value of 4 in P2 euploid mice reached a value of 7 in P8 euploid mice. In P2 mice, there were no genotype-related differences in the maximum number of dendritic orders (Fig. 4d–f), mean length of branches of order 1–3 (Fig. 4d), mean number of branches of each dendritic order (Fig. 4e), and total length of each dendritic order (Fig. 4f). The only genotype-related difference regarded the mean length of branches of order 4 that was significantly smaller in Ts65Dn in comparison with euploid mice (Fig. 4d). At P8, while euploid mice had apical branches up to order 7, in Ts65Dn mice, branches of this order were missing (Fig. 4j–l). In addition, Ts65Dn mice aged 8 days had a reduced number (Fig. 4k) and total length (Fig. 4l) of branches of order >3, although this difference was not statistically significant or only approached statistical significance for the number of branches of orders 4 and 5. Observation of the scatterplots in Figure 4d, e, j–l shows that measurements of number and length of high-order apical branches exhibited large interindividual differences both in euploid and Ts65Dn mice. This was true also for high-order collateral and basal branches (see below: Fig. 5d, e, j–l, 6d, e, j–l). It seems of relevance to note that this large variance is suggestive of large interindividual differences in the rate of dendritic maturation, on the one hand, and, on the other hand, it may hamper detection of statistically significant differences across groups.

These results show a reduction in the length of the highest order apical branches (order 4) in the pyramidal neurons of the frontal cortex of P2 Ts65Dn mice and that more widespread defects begin to appear at the level of high-order apical branches (orders 4–7) when Ts65Dn mice reach the age of 8 days.

Quantification of the Collateral Dendrites of Pyramidal Neurons in P2 and P8 Euploid and Ts65Dn Mice

An evaluation of the collateral dendrites of P2 mice showed that the total length (Fig. 5a), number of branches (Fig. 5b), and mean branch length (Fig. 5c) were smaller in Ts65Dn in comparison with euploid mice, although these differences were not statistically significant. Detailed analysis of each order of the collateral dendrites showed no statistically significant difference between Ts65Dn and euploid mice in the mean length (Fig. 5d), mean number (Fig. 5e), and total length (Fig. 5f) of branches of orders 1 and 2, although in absolute terms, the mean length (Fig. 4d), mean number (Fig. 5e), and total length (Fig. 5f) of branches of order 2 were notably smaller in Ts65Dn in comparison with euploid mice. Unlike euploid mice, Ts65Dn mice completely lacked branches of order 3 (Fig. 5d–f: black arrows).

An evaluation of the collateral dendrites of P8 mice showed Ts65Dn mice had collateral dendrites with a total length (Fig. 5g) and mean branch length (Fig. 5i) like those of their euploid counterparts but a significantly larger number of branches in comparison with euploid mice (Fig. 5h). Detailed analysis of each order showed that unlike for the apical branches, in the case of collateral branches, there was no age-related increase in the number of orders that had a value of 3 both in P8 (Fig. 5j–l) and P2 (Fig. 5d–f) euploid mice. While at P2 Ts65Dn mice completely lacked branches of order 3 (Fig. 4d–f: black arrow), this defect disappeared at P8 (Fig. 5j–l). Analysis of each order showed no statistically significant differences between P8 Ts65Dn and euploid mice in the mean branch length (Fig. 5j) and total order length (Fig. 5l). The number of branches of order 1 however was significantly larger in Ts65Dn than in euploid mice (Fig. 5k).

These results show lack of high-order collateral branches in Ts65Dn mice aged 2 days but that this defect disappears when mice reach the age of 8 days. Moreover, at the age of 8 days, Ts65Dn mice have even more collateral dendrites than their euploid counterparts.

Quantification of the Basal Dendrites of Pyramidal Neurons in P2 Euploid and Ts65Dn Mice

An evaluation of the basal dendrites showed that at P2, Ts65Dn mice had a significantly reduced total length (−44%; Fig. 6a) and a reduced mean branch length (−34%; Fig. 6c) in comparison with their euploid counterparts. In addition, Ts65Dn mice had fewer branches (−18%; Fig. 6b), although this difference was not statistically significant. Detailed analysis of each order of the basal dendrites showed that in Ts65Dn mice, the length of branches of orders 1 and 2 was significantly smaller (−41% and −28%, respectively) in comparison with euploid mice (Fig. 6d). Moreover, unlike euploid mice, Ts65Dn mice lacked branches of orders 3 and 4 (Fig. 6d–f: black arrows). In addition, Ts65Dn mice had fewer branches of order 2 (−26%), although the difference was not statistically significant. The total length of orders 1 and 2 was reduced (−27% and −58%, respectively) in Ts65Dn in comparison with euploid mice, and this difference was statistically significant in the case of order 2 (Fig. 6f).

An evaluation of the total length, number of branches, and mean branch length of the apical dendritic branches of P8 mice showed no genotype-related differences (Fig. 6g–i). P8 euploid mice exhibited an increase in the number of basal dendritic orders that from a value of 4 in P2 euploid mice reached a value of 5 in P8 mice. While P2 Ts65Dn mice lacked branches of orders 3 and 4 (Fig. 6d– f: black arrow), this defect disappeared in P8 Ts65Dn mice (Fig. 6j–l). Detailed analysis of each order in P8 mice showed no statistically significant differences between Ts65Dn and euploid mice in the mean branch length (Fig. 6j), mean number of branches (Fig. 6k), and total length (Fig. 6l) of branches of each order. These results show that the basal dendritic tree of the pyramidal neurons of layer II/III is hypotrophic in Ts65Dn mice aged 2 days in comparison with their euploid counterparts but that this defect disappears with age.

Size of the Cell Body of Pyramidal Neurons in P2 and P8 Euploid and Ts65Dn Mice

An evaluation of the geometry of the cell body of the sampled neurons showed no statistically significant differences between Ts65Dn and euploid mice in the surface area and long axis both at P2 (Fig. 7b, c) and P8 (Fig. 7e, f). The short axis, however, was significantly smaller in Ts65Dn mice in comparison with their euploid counterparts both at P2 (Fig. 7c) and P8 (Fig. 7f). Consequently, at both ages, the ratio between the long and short axis was larger in Ts65Dn mice in comparison with their euploid counterparts (Fig. 7d, g).

Spine Density on Pyramidal Neurons of P2 and P8 Euploid and Ts65Dn Mice

As mentioned above, pyramidal neurons of P2 mice exhibited spines on the soma but not on the apical and basal dendrites. Spines however were detectable on the dendritic branches of pyramidal neurons of mice aged 8 days. An

evaluation of the density of somatic spines in P2 mice showed no statistically significant difference between Ts65Dn and euploid mice (Fig. 7i). An evaluation of spine density on the basal dendritic branches of P8 mice showed no genotype-related significant differences in spine density (Fig. 7k).

Discussion

Developmental Changes in Layer II/III Pyramidal Neurons of the Frontal Cortex

We found here that pyramidal neurons in layer II/III of the frontal cortex of euploid mice aged 2 days had apical and basal dendritic branches up to order 4. In the sensorimotor cortex of rats aged 3 days, pyramidal neurons of layer V have apical and basal branches up to orders 3 and 4, respectively [35], which fits with our data in pyramidal neurons of layer II/III of P2 mice. Results showed that the number of apical and basal branches, but not of collateral branches, exhibited an increase from the age of 2 days to the age of 8 days. The increase was proportionally larger in the apical tree (from 4 branches in P2 mice to 7 branches in P8 mice; a 1.75-times increase) in comparison with basal tree (from 4 branches in P2 mice to 5 branches in P8 mice; a 1.25-times increase) suggesting a delayed and possibly more prolonged development of the apical dendritic arbor. This seems to be consistent with evidence showing that development of the basal and apical dendritic arbors of CA1 pyramidal neurons has a different time course; the number of basal dendrites is established already at the age of 5 days, while lateral and terminal branches of the apical arbor emerge later [36]. In agreement with other studies [29–32], we found the absence of dendritic spines at the age of 2 days but that at 8 days of age, dendritic spines were present on all dendritic arbors.

Different Development of Pyramidal Neurons in the Frontal Cortex of Ts65Dn and Euploid Mice

A comparison of the pyramidal neurons of Ts65Dn and euploid mice at P2 and P8 showed early differences in the dendritic branching pattern. As discussed below, these changes were related to both dendritic compartment and age.

Almost no abnormalities were present in the size and geometry of the apical dendritic arbor of P2 Ts65Dn mice. The pyramidal neurons of Ts65Dn mice aged 8 days however had an apical tree less developed in comparison with that of euploid mice of the same age because it had high order branches that were shorter and reduced in number and lacked branches of the highest order (order 7). No study has quantified the apical dendritic arborization in the frontal cortex (and other cortical areas) of adult Ts65Dn mice. It remains to be established whether the hypotrophy of the apical arbor found here in the frontal cortex of Ts65Dn mice aged 8 days further deteriorates with age. It is known however that the dendritic arbor of the granule cells, which corresponds to the apical arbor of neurons endowed with both basal and apical dendrites [37], is notably hypotrophic at 8 days and at older ages [20, 38, 39]. This indicates that at least in the hippocampal region, the apical arborization of Ts65Dn mice is hypotrophic starting at 8 days of age and that this defect is retained in adulthood.

In P2 mice, the collateral dendrites emerging from the main apical shaft lacked branches of order 3, but this defect was no longer present in P8 mice that, additionally, exhibited more branches of order 1 in comparison with their euploid counterparts, suggesting an age-related mechanism of overcompensation in this dendritic domain. This finding appears in line with evidence showing that in children with DS, the number of dendritic branches of pyramidal neurons is even above normal in the infantile period (6 months old or less) but drops steadily to below normal in infants older than 2 years [13].

Unlike the apical dendritic tree, the basal dendritic tree of Ts65Dn mice aged 2 days already exhibited various defects in comparison with euploid mice of the same age. The most patent defect was the lack of high-order branches. In addition, branches of orders 1 and 2 were shorter in comparison with those of euploid mice. Altogether, these defects caused a reduction of the total length of the basal dendritic tree. In contrast, the basal dendritic arbor of P8 Ts65Dn mice had a pattern like that of their euploid counterparts, suggesting that the early defects of the basal dendritic tree present at P2 are compensated when mice reach the age of 8 days. It must be noted however that analysis of the basal dendritic arbor of layer III pyramidal neurons in the frontal cortex of adult Ts65Dn mice showed that they have notably fewer branches and a reduced length in comparison with euploid mice [40]. Taken together, these data suggest that (i) a trisomy-related defect is present in the basal dendritic arbor of pyramidal neurons that manifest itself at P2, (ii) some forms of compensation take place between P2 and P8, and (iii) this compensation is not sufficient to ensure a proper development at further life stage which renders the basal arbor of adult Ts65Dn mice

hypotrophic in comparison with that of euploid mice.

Taken together, our results show that while very precocious defects are present in the basal tree of Ts65Dn mice, defects in the apical tree start to appear slightly later in development. This suggests that trisomy-linked defects in dendritic development are temporally shifted with respect to the dendritic date of birth. In addition, results suggest that these dendritic defects may dynamically change over time. The process of dendritogenesis is controlled by an intrinsic genetic program and extracellular signals [41]. The mechanisms whereby trisomy affects dendritic development remain elusive. The triplicated genes DS cell-adhesion molecule and dual-specificity tyrosine-phosphorylated and regulated kinase 1A are likely to be critical determinants of improper dendritic development in DS in view of their established role in dendritic development [20, 42–45]. Specific studies are required to determine the role of these and, possibly, other genes in the regulation of dendritic development during different developmental time points in the DS brain. Dendritic morphology determines the computations a neuron can perform and has a role in circuit function. The hypotrophy of the dendritic domains of pyramidal neurons of Ts65Dn pups implies differences in dendritic electrotonic properties that, in turn, are likely to cause changes in neuronal excitability. Moreover, at both ages examined here, pyramidal neurons of the frontal cortex had a soma with a smaller width in Ts65Dn in comparison with euploid mice which may also contribute to affect neuron excitability. For instance, computational modeling demonstrates that the somatodendritic morphology will dictate excitability changes occurring in response to changes in the plasticity of the axon initial segment [46]. The reduction in dendritic complexity observed here in trisomic neurons signifies reduction in excitatory postsynaptic responses as well as dendritic space constant, with consequent reduction in firing probability [47]. This, in turn, implies impoverishment of communications among neurons and, consequently, of brain functioning. The early appearance of dendritic changes in the DS cortex may concur, by adding to the typical neuronal poverty of this pathology, to undermine development of cognitive functions from very early life stages.

Absence of Differences in Spine Density in Pyramidal Neurons of the Frontal Cortex of P2 and P8 Ts65Dn Mice

We found that in P2 mice spines were present on the soma of pyramidal neurons but not on the dendrites. Somatic spines are a transient feature of immature neocortical pyramidal [30, 33] and hippocampal [34] neurons, but very few persist into maturity. One type of somatic spine forms synapses with axons passing the cell, and the other, without synapses, appears to serve as a buttress for neuronal and glial processes [48]. We found no differences between P2 Ts65Dn and euploid mice in the density of somatic spines. Likewise, an evaluation of basal dendritic spines in P8 mice showed no genotype-related differences. Previous evidence showed no differences in dendritic spine density in the hippocampus of Ts65Dn and euploid mice aged 8 days [39], but a severe spine density reduction was detected in the hippocampus of Ts65Dn mice aged 15 days [49] and in the hippocampus [19–22] and neocortex [2] of adult Ts65Dn mice. Taken together, these data show that, similarly to defects in dendritic arborization, defects in spinogenesis are a relatively late occurring event in Ts65Dn mice. These observations are in agreement with the lack of differences in dendritic spine density in fetuses and young infants with DS and the appearance of spine density defects at later life stages [12]. This knowledge provides a window of opportunity for treatment aimed at ameliorating spine development in DS.

Concluding Remarks

Dendritic pathology is one of the typical phenotypic features of DS. The dendrites of fetuses and newborns with DS are normal in their appearance but begin to differ from those of normally developing children in the first months of age [12–16]. We found here that neocortical pyramidal neurons of Ts65Dn pups exhibit dendritic defects involving both the basal and apical dendrites. These defects, however, are relatively mild in comparison with those observed in adult mice [2, 19–22]. The lack of a severe dendritic pathology in Ts65Dn pups is reminiscent of the absence of dendritic alterations in fetuses with DS and the appearance of dendritic defects during early infancy only. Thus, similarly to individuals with DS, it appears that in Ts65Dn mice, defective dendritic formation takes place progressively during ontogenesis. Knowledge of the timeline of dendritic pathology in humans (and mouse models) provides the opportunity to try to interrupt and reverse it pharmacologically. The similarity in the establishment of dendritic defects between humans and the Ts65Dn mouse validates the Ts65Dn mouse as a useful model to dissect the mechanisms of dendritic developmental abnormalities in DS and test therapeutic interventions.

Acknowledgment

We thank Francesco Campisi for his technical assistance.

Statement of Ethics

Experiments were performed in accordance with the European Communities Council Directive of 24 November 1986 (86/609/EEC) for the use of experimental animals. This study protocol was reviewed and approved by Italian Ministry of Public Health (205/2019-PR).

Conflict of Interest Statement

The authors declare that they have no conflict of interest.

Funding Sources

This work was supported by a grant to R.B. from "Fondazione Generali e Assicurazione Generali," Italy.

Author Contributions

B.U. carried out histology, analyzed dendritic arborization of mice aged 2 days, and was involved in drafting the manuscript. F.S. carried out histology, analyzed dendritic arborization of mice aged 8 days, and was involved in drafting the manuscript. M.E. carried out statistical analysis and prepared the figures. A.G. carried out statistical analysis and prepared the figures. C.R. analyzed dendritic spine density. S.G. carried out histology and was involved in drafting the manuscript. R.B. conceived the study and wrote the article.

Data Availability Statement

The data that support the findings of this study are available from the corresponding author upon reasonable request.

References

1 Kaufmann WE, Moser HW. Dendritic anomalies in disorders associated with mental retardation. Cereb Cortex. 2000 Oct;10(10): 981–91.
2 Benavides-Piccione R, Ballesteros-Yanez I, de Lagran MM, Elston G, Estivill X, Fillat C, et al. On dendrites in Down syndrome and DS murine models: a spiny way to learn. Prog Neu- robiol. 2004 Oct;74(2):111–26.
3 Dierssen M, Ramakers GJ. Dendritic pathology in mental retardation: from molecular genetics to neurobiology. Genes Brain Behav. 2006;5 Suppl 2:48–60.
4 Granato A, Merighi A. Dendrites of neocortical pyramidal neurons: the key to understand intellectual disability. Cell Mol Neurobiol. 2021 Jul 3. Epub ahead of print.
5 Quach TT, Stratton HJ, Khanna R, Kolattukudy PE, Honnorat J, Meyer K, et al. Intellectual disability: dendritic anomalies and emerging genetic perspectives. Acta Neuro- pathol. 2021 Feb;141(2):139–58.
6 Stagni F, Giacomini A, Emili M, Guidi S, Bartesaghi R. Neurogenesis impairment: an early developmental defect in Down syndrome. Free Radic Biol Med. 2018;114:15–32.
7 Bartesaghi R, Guidi S, Ciani E. Is it possible to improve neurodevelopmental abnormalities in Down syndrome? Rev Neurosci. 2011; 22(4):419–55.
8 Suetsugu M, Mehraein P. Spine distribution along the apical dendrites of the pyramidal neurons in Down's syndrome. A quantitative Golgi study. Acta Neuropathol. 1980;50(3): 207–10.
9 Takashima S, Ieshima A, Nakamura H, Becker LE. Dendrites, dementia and the Down syndrome. Brain Dev. 1989;11(2):131–3.
10 Ferrer I, Gullotta F. Down's syndrome and Alzheimer's disease: dendritic spine counts in the hippocampus. Acta Neuropathol. 1990; 79(6):680–5.
11 Takashima S, Iida K, Mito T, Arima M. Dendritic and histochemical development and ageing in patients with Down's syndrome. J Intellect Disabil Res. 1994 Jun;38 (Pt 3):265– 73.
12 Takashima S, Becker LE, Armstrong DL, Chan F. Abnormal neuronal development in the visual cortex of the human fetus and infant with Down's syndrome. A quantitative and qualitative Golgi study. Brain Res. 1981 Nov 23;225(1):1–21.
13 Becker LE, Armstrong DL, Chan F. Dendritic atrophy in children with Down's syndrome. Ann Neurol. 1986 Oct;20(4):520–6.
14 Prinz M, Prinz B, Schulz E. The growth of non-pyramidal neurons in the primary motor cortex of man: a Golgi study. Histol Histo- pathol. 1997 Oct;12(4):895–900.
15 Schulz E, Scholz B. [Neurohistological findings in the parietal cortex of children with chromosome aberrations]. J Hirnforsch. 1992;33(1):37–62. German.
16 Vuksic M, Petanjek Z, Rasin MR, Kostovic I. Perinatal growth of prefrontal layer III pyramids in Down syndrome. Pediatr Neurol. 2002 Jul;27(1):36–8.
17 Herault Y, Delabar JM, Fisher EMC, Tybulewicz VLJ, Yu E, Brault V. Rodent models in Down syndrome research: impact and future opportunities. Dis Model Mech. 2017 Oct 1; 10(10):1165–86.
18 Rueda N, Flórez J, Martínez-Cué C. Mouse models of Down syndrome as a tool to unravel the causes of mental disabilities. Neural Plast. 2012;2012:584071.
19 Belichenko PV, Masliah E, Kleschevnikov AM, Villar AJ, Epstein CJ, Salehi A, et al. Synaptic structural abnormalities in the Ts65Dn mouse model of Down

syndrome. J Comp Neurol. 2004 Dec 13;480(3):281–98.
20 Guidi S, Stagni F, Bianchi P, Ciani E, Ragazzi E, Trazzi S, et al. Early pharmacotherapy with fluoxetine rescues dendritic pathology in the Ts65Dn mouse model of Down syndrome. Brain Pathol. 2013;23(2):129–43.
21 Dang V, Medina B, Das D, Moghadam S, Martin KJ, Lin B, et al. Formoterol, a longacting beta2 adrenergic agonist, improves cognitive function and promotes dendritic complexity in a mouse model of Down syndrome. Biol Psychiatry. 2014 Feb 1;75(3): 179–88.
22 Stagni F, Giacomini A, Guidi S, Ciani E, Ragazzi E, Filonzi M, et al. Long-term effects of neonatal treatment with fluoxetine on cognitive performance in Ts65Dn mice. Neurobiol Dis. 2015 Feb;74:204–18.
23 Uguagliati B, Al-Absi AR, Stagni F, Emili M, Giacomini A, Guidi S, et al. Early appearance of developmental alterations in the dendritic tree of the hippocampal granule cells in the Ts65Dn model of Down syndrome. Hippo- campus. 2021 Apr;31(4):435–47.
24 Petrides M, Alivisatos B, Evans AC, Meyer E. Dissociation of human mid-dorsolateral from posterior dorsolateral frontal cortex in memory processing. Proc Natl Acad Sci U S A. 1993 Feb 1;90(3):873–7.
25 Vicari S, Pontillo M, Armando M. Neurodevelopmental and psychiatric issues in Down's syndrome: assessment and intervention. Psy- chiatr Genet. 2013 Jun;23(3):95–107.
26 Reinholdt LG, Ding Y, Gilbert GJ, Czechanski A, Solzak JP, Roper RJ, et al. Molecular characterization of the translocation breakpoints in the Down syndrome mouse model Ts65Dn. Mamm Genome. 2011 Dec;22(11–12): 685–91.
27 Paxinos G, Halliday G, Watson C, Koutcherov Y, Wang H. Atlas of the developing mouse brain. Academic Press, Elsevier; 2007. p. 356.
28 Kuehne CC. The advantages of using planned comparisons over post hoc tests [microform]. ERIC Clearinghouse; 1993.Meller K, Breipohl W, Glees P. Ontogeny of the mouse motor cortex. The polymorph layer or layer VI. A Golgi and electronmicroscopical study. Z Zellforsch Mikrosk Anat. 1969;99(3):443–58.
29 Juraska JM, Fifkova E. A Golgi study of the early postnatal development of the visual cortex of the hooded rat. J Comp Neurol. 1979 Jan 15;183(2):247–56.
30 Yuste R, Bonhoeffer T. Genesis of dendritic spines: insights from ultrastructural and imaging studies. Nat Rev Neurosci. 2004 Jan; 5(1):24–34.
31 Romand S, Wang Y, Toledo-Rodriguez M, Markram H. Morphological development of thick-tufted layer v pyramidal cells in the rat somatosensory cortex. Front Neuroanat. 2011;5:5.
32 Juraska JM, Fifkova E. An electron microscope study of the early postnatal development of the visual cortex of the hooded rat. J Comp Neurol. 1979 Jan 15;183(2):257–67.
33 Seay-Lowe SL, Claiborne BJ. Morphology of intracellularly labeled interneurons in the dentate gyrus of the immature rat. J Comp Neurol. 1992 Oct 1;324(1):23–36.
34 Petit TL, LeBoutillier JC, Gregorio A, Libstug
H. The pattern of dendritic development in the cerebral cortex of the rat. Brain Res. 1988 Jun 1;469(1–2):209–19.
35 Pokorny J, Yamamoto T. Postnatal ontogenesis of hippocampal CA1 area in rats. I. Development of dendritic arborisation in pyramidal neurons. Brain Res Bull. 1981;7:113–20.
36 Wu YK, Fujishima K, Kengaku M. Differentiation of apical and basal dendrites in pyramidal cells and granule cells in dissociated hippocampal cultures. PLoS One. 2015;10(2): e0118482.
37 Emili M, Stagni F, Salvalai ME, Uguagliati B, Giacomini A, Albac C, et al. Neonatal therapy with clenbuterol and salmeterol restores spinogenesis and dendritic complexity in the dentate gyrus of the Ts65Dn model of Down syndrome. Neurobiol Dis. 2020 Jul; 140: 104874.
38 Uguagliati B, Al-Absi AR, Stagni F, Emili M, Giacomini A, Guidi S, et al. Early appearance of developmental alterations in the dendritic tree of the hippocampal granule cells in the Ts65Dn model of Down syndrome. Hippo- campus. 2021 Apr;31(4):435–47.Dierssen M, Benavides-Piccione R, MartinezCue C, Estivill X, Florez J, Elston GN, et al. Alterations of neocortical pyramidal cell phenotype in the Ts65Dn mouse model of Down syndrome: effects of environmental enrichment. Cereb Cortex. 2003 Jul;13(7):758–64.
39 Urbanska M, Blazejczyk M, Jaworski J. Molecular basis of dendritic arborization. Acta Neurobiol Exp. 2008;68(2):264–88.
40 Alves-Sampaio A, Troca-Marín JA, Montesinos ML. NMDA-mediated regulation of DSCAM dendritic local translation is lost in a mouse model of Down's syndrome. J Neuro- sci. 2010 Oct 6;30(40):13537–48.
41 Martinez de Lagran M, Benavides-Piccione R, Ballesteros-Yanez I, Calvo M, Morales M, Fillat C, et al. Dyrk1A influences neuronal morphogenesis through regulation of cytoskeletal dynamics in mammalian cortical neurons. Cereb Cortex. 2012 Dec;22(12):2867–77.
42 Ori-McKenney KM, McKenney RJ, Huang HH, Li T, Meltzer S, Jan LY, et al. Phosphorylation of beta-Tubulin by the Down syndrome kinase, minibrain/DYRK1a, regulates microtubule dynamics and dendrite morphogenesis. Neuron. 2016 May 4;90(3):551–63.
43 Santos RA, Fuertes AJC, Short G, Donohue KC, Shao H, Quintanilla J, et al. DSCAM differentially modulates preand postsynaptic structural and functional central connectivity during visual system wiring. Neural Dev. 2018 Sep 15;13(1):22.
44 Gulledge AT, Bravo JJ. Neuron morphology influences axon initial segment plasticity. eN- euro. 2016 Jan–Feb;3(1).
45 Kirch C, Gollo LL. Single-neuron dynamical effects of dendritic pruning implicated in aging and neurodegeneration: towards a measure of neuronal reserve. Sci Rep. 2021 Jan 14; 11(1):1309.
46 Ifft JD, McCarthy L. Somatic spines in the supraoptic nucleus of the rat hypothalamus. Cell Tissue Res. 1974 Apr 11;148(2):203–11.
47 Stagni F, Giacomini A, Guidi S, Emili M, Uguagliati B, Salvalai ME, et al. A flavonoid agonist of the TrkB receptor for BDNF improves hippocampal neurogenesis and hippocampus-dependent memory in the Ts65Dn mouse model of DS. Exp Neurol. 2017 Sep 4; 298(Pt A):79–96.
48 Ifft JD, McCarthy L. Somatic spines in the supraoptic nucleus of the rat hypothalamus. Cell Tissue Res. 1974 Apr 11; 148(2): 203–11.
49 Stagni F, Giacomini A, Guidi S, Emili M, Uguagliati B, Salvalai ME, et al. A flavonoid agonist of the TrkB receptor for BDNF im-proves hippocampal neurogenesis and hippo-campus-dependent memory in the Ts65Dn mouse model of DS. Exp Neurol. 2017 Sep 4; 298(Pt A): 79–96.

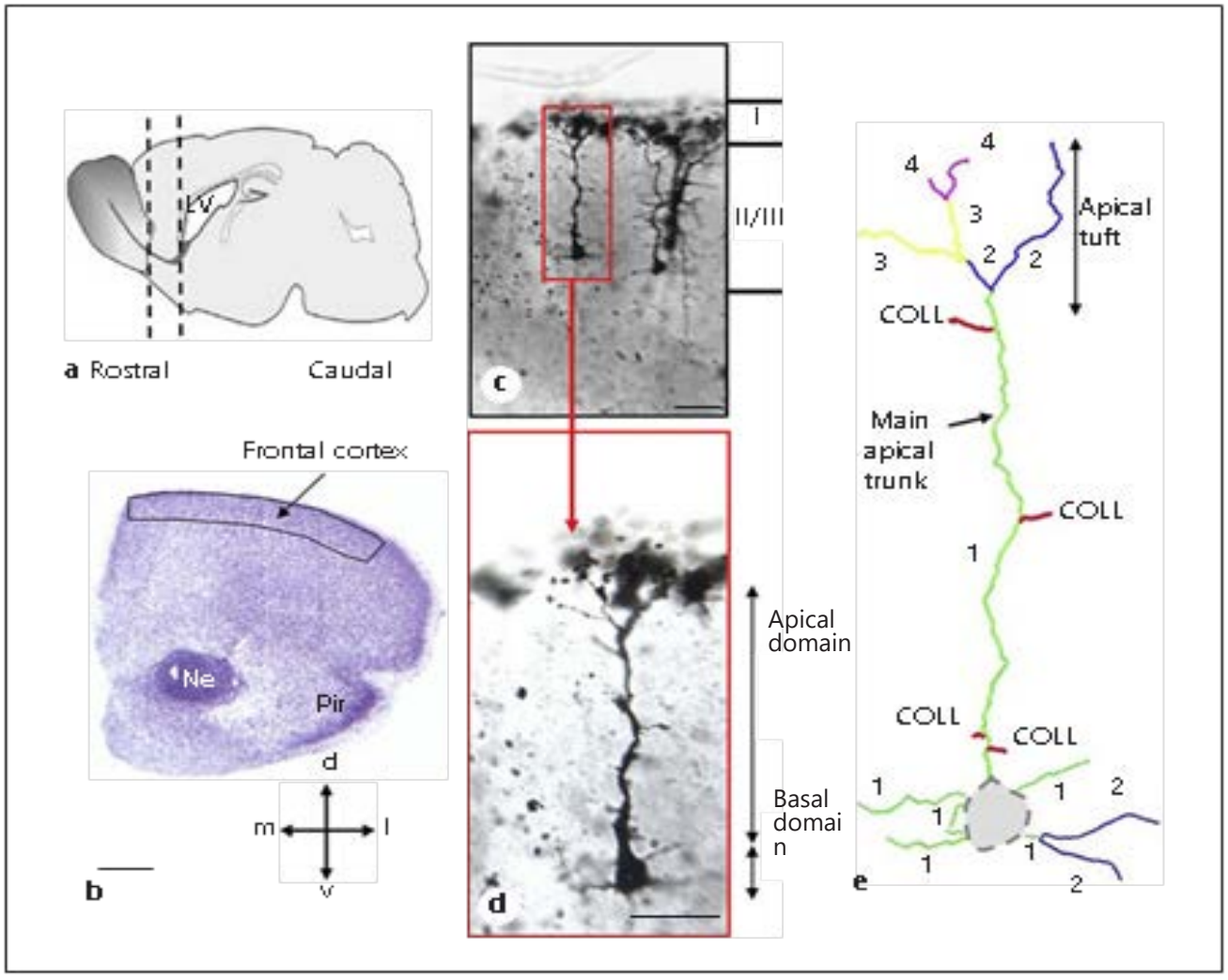

Fig. 1. Experimental protocol. **a** Schematic drawing of a lateral view of the mouse brain showing the borders of the frontal lobe region where neurons were sampled. **b** Nissl stained coronal section across the frontal lobe of a P2 mouse showing the area of the frontal cortex where neurons were sampled. **c** Micrograph of a Golgi-stained brain section showing examples of pyramidal neurons in layer II/III of P2 mice. The roman numerals indicate cortical layers I and II/III. **d** Higher magnification image of the boxed area in (**c**). Calibration bar in (**b**), 200 μm, in (**c**, **d**), 40 μm. **e** Computerized reconstruction of the dendritic arbor of pyramidal neurons. Dendrites were traced in a centrifugal direction. Numbers indicate the different dendritic orders (marked by the software with different colors). COLL, collateral dendrites; d, dorsal; l, lateral; m, medial; Ne, neuroepithelium; Pir, piriform cortex; v, ventral.

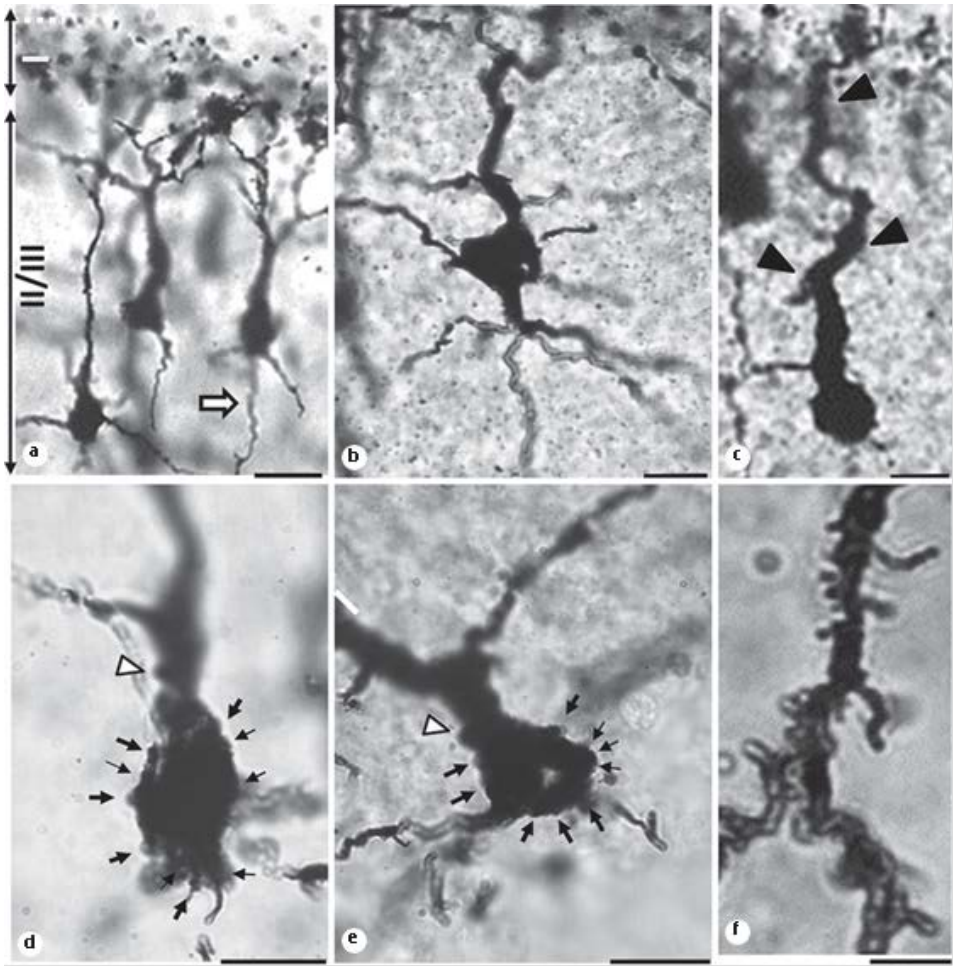

Fig. 2. Examples of Golgi-stained neurons in layer II/III of the frontal cortex. **a** Examples of neurons of a P2 mouse with cell body at a different distance from layer I. All neurons send their apical dendrites toward layer I. The neuron on the right has an axon (empty arrow) directed toward the deep layers. The roman numerals indicate cortical layers I and II/III. **b**, **c** Example of a relatively mature (**b**) and a more immature pyramidal neuron in P2 mice (**c**). The black arrowheads in (**c**) indicate varicosities along the shaft of the apical dendrite. **d**, **e** High magnification micrograph of neurons of layer II/III of P2 mice showing spines (arrows) on the soma. Spines were occasionally found on the portion of the primary apical dendrite close to the soma (white arrowhead). Notice the absence of spines on more distal portion of the primary apical dendrite (**d**, **e**), its branches (**d**), and on the basal dendrites (**e**). **f** High magnification micrograph of basal dendrites of a neuron in layer II/III of a P8 mouse, showing the presence of spines on the basal dendrites. Calibrations bar in (**a**), 20 μm, in (**b–f**), 10 μm.

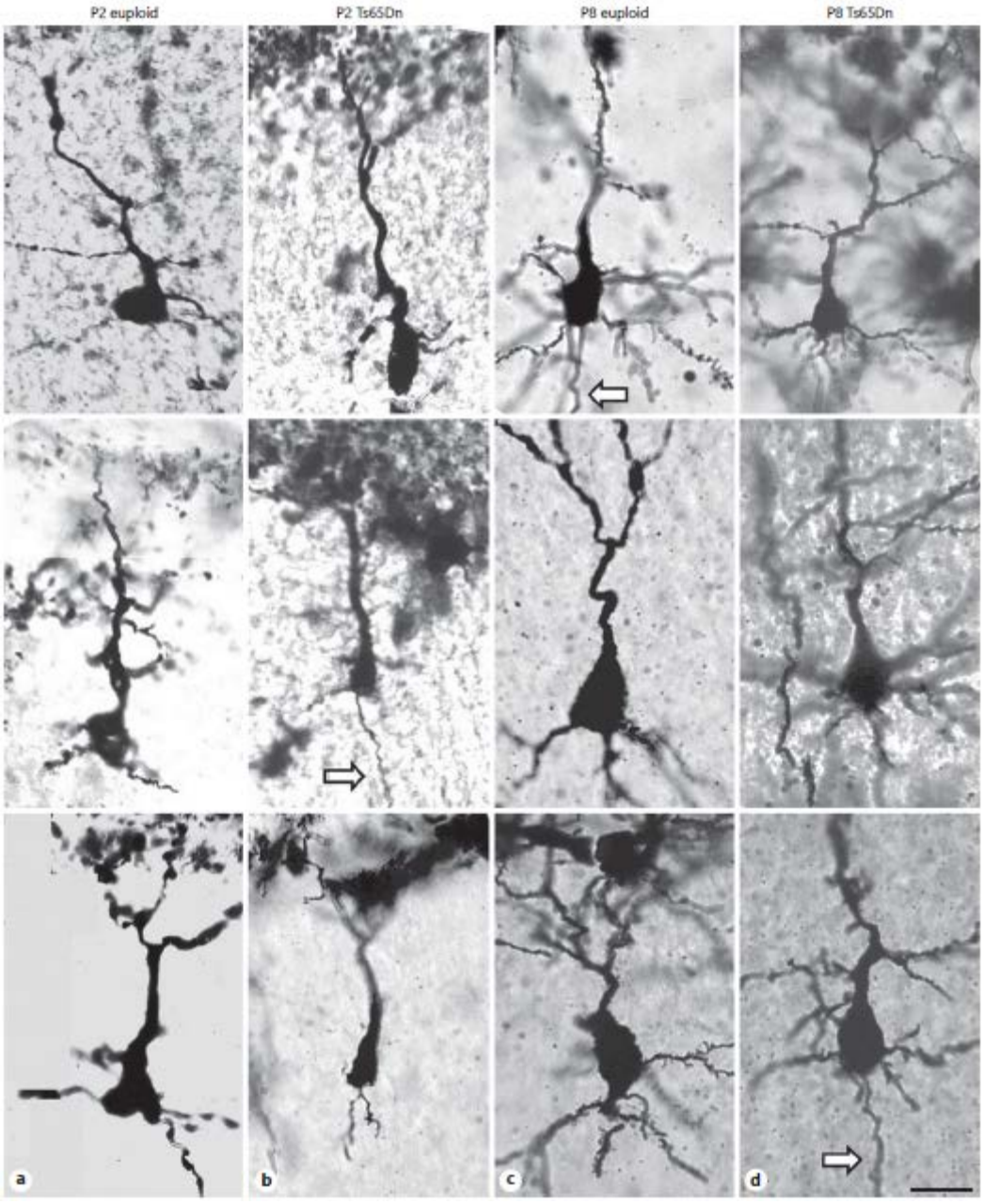

Fig. 3. Examples of Golgi-stained neurons in layer II/III of the frontal cortex of P2 and P8 euploid and Ts65Dn mice. a–d Each column reports examples of pyramidal neurons of the frontal cortex of P2 euploid (a) and Ts65Dn (b) mice and P8 euploid (c) and Ts65Dn (d) mice, as indicated at the top of the columns. The empty arrows indicate axons irected toward the deep layers. Calibration bar, 20 μm.

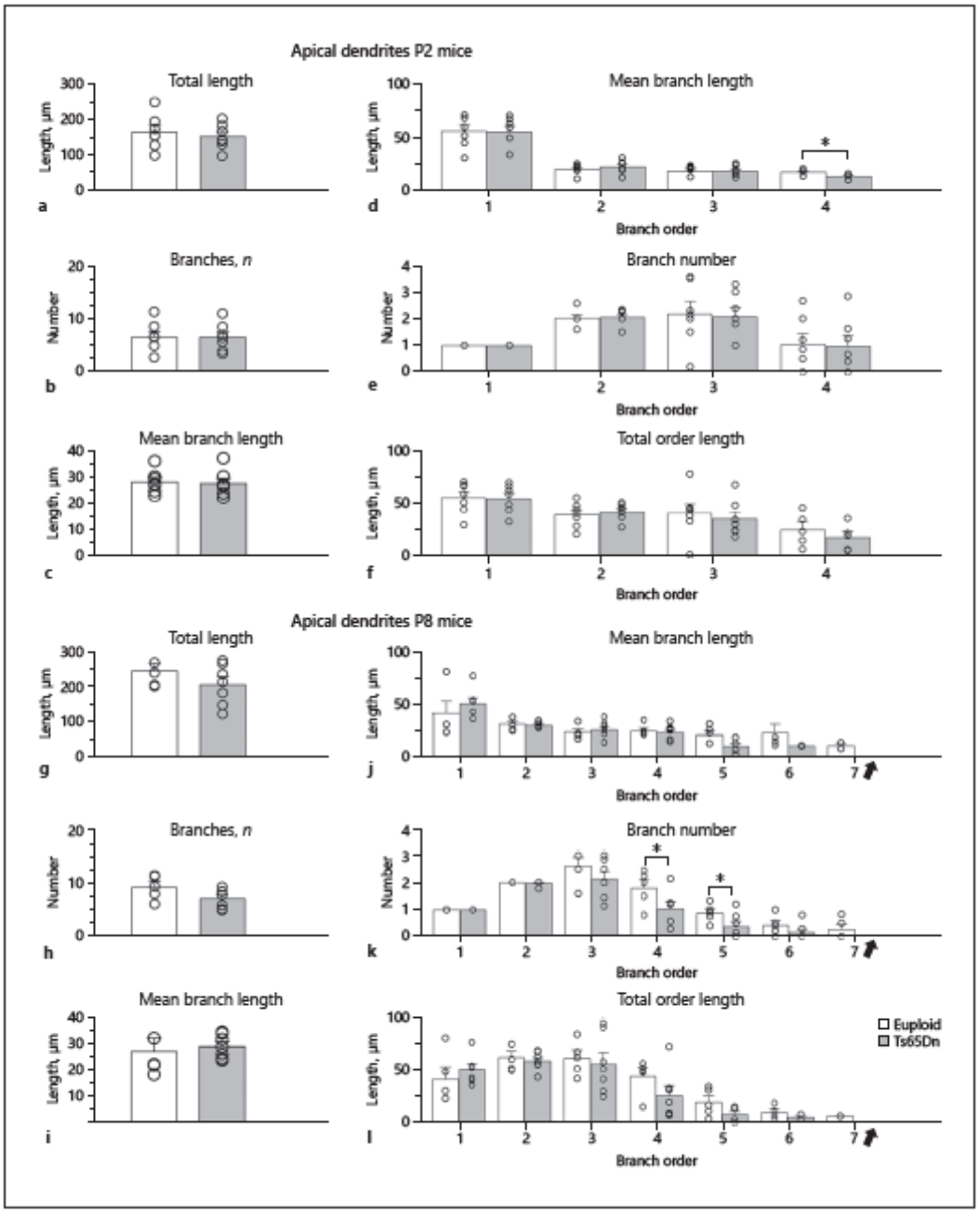

Fig. 4. Morphometry of the apical dendrites of pyramidal neurons in layer II/III of the frontal cortex of P2 and P8 euploid and Ts65Dn mice. a–c Quantification of the total length (a), total number of branches (b), and mean branch length (c) in P2 mice. d–f Quantification of the mean length (d), total number (e), and total length (f) of branches of each order in P2 mice. g–i Quantification of the total length (g), total number of branches (h), and mean branch length (i) in P8 mice. j–l Quantification of the mean length (j), total number (k), and total length (l) of branches of each order in P8 mice. Values in (a–l) represent mean ± SE. The scatterplots over each column represent the values of individual cases for each group. The black arrow in (j–l) indicates lack of branches of order 7 in P8 Ts65Dn mice. *p = 0.06; *p < 0.05; Student's t test or MannWhitney U test.

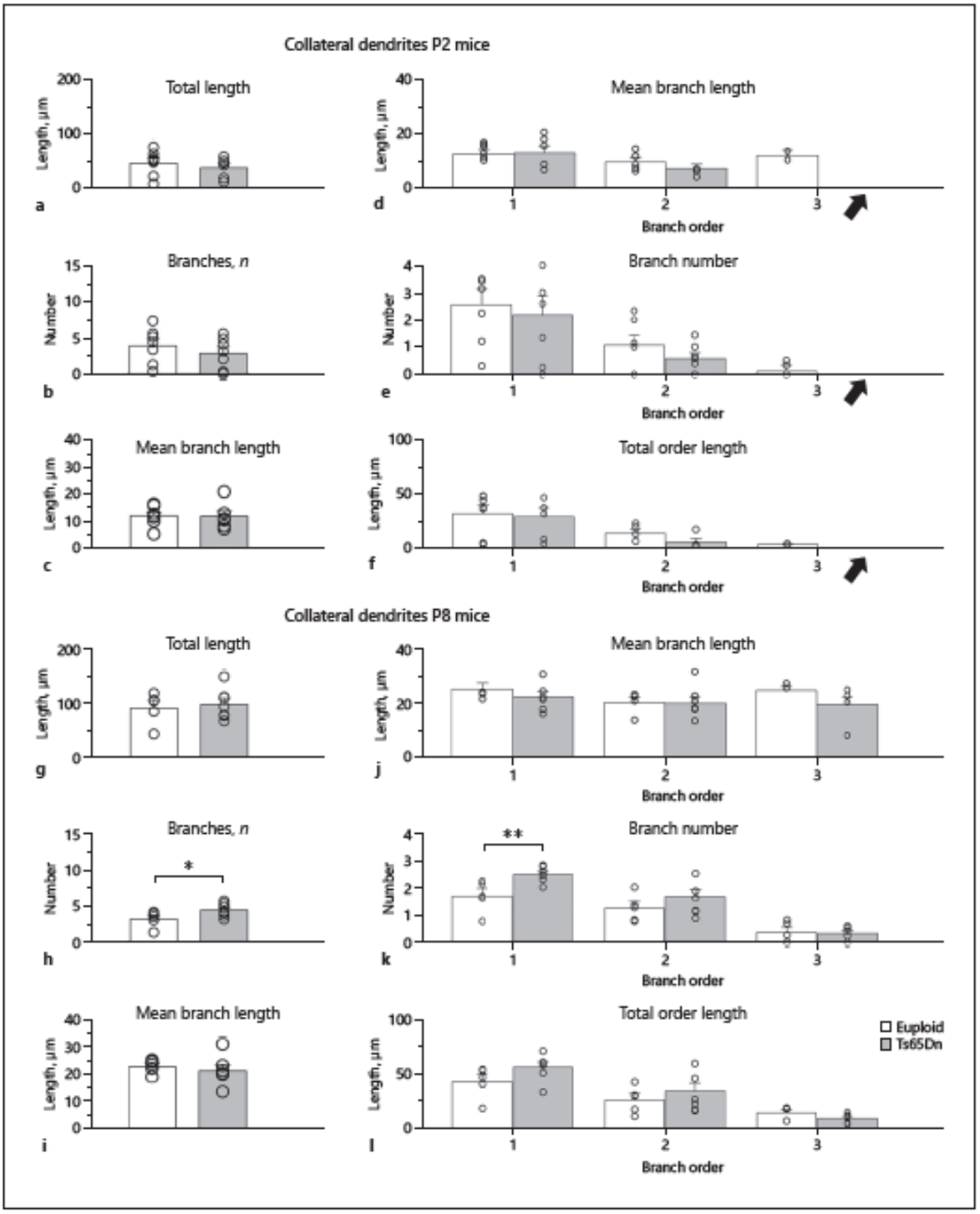

593
594 **Fig. 5**. Morphometry of the collateral dendrites of pyramidal neurons in layer II/III of the frontal cortex of P2 and P8
595 euploid and Ts65Dn mice. a–c Quantification of the total length (a), total number of branches (b), and mean branch
596 length (c) in P2 mice. d–f Quantification of the mean length (d), total number (e), and total length (f) of branches of
597 each order in P2 mice. g–i Quantification of the total length (g), total number of branches (h), and mean branch length
598 (i) in P8 mice. j–l Quantification of the mean length (j), total number (k), and total length (l) of branches of each order
599 in P8 mice. Values in (a–l) represent mean ± SE. The scatterplots over each column represent the values of individual
600 cases for each group. The black arrow in (d–f) indicates lack of branches of order 3 in P2 Ts65Dn mice. *p = 0.06;
601 **p < 0.01; Student's t test or Mann-Whitney U test.
602

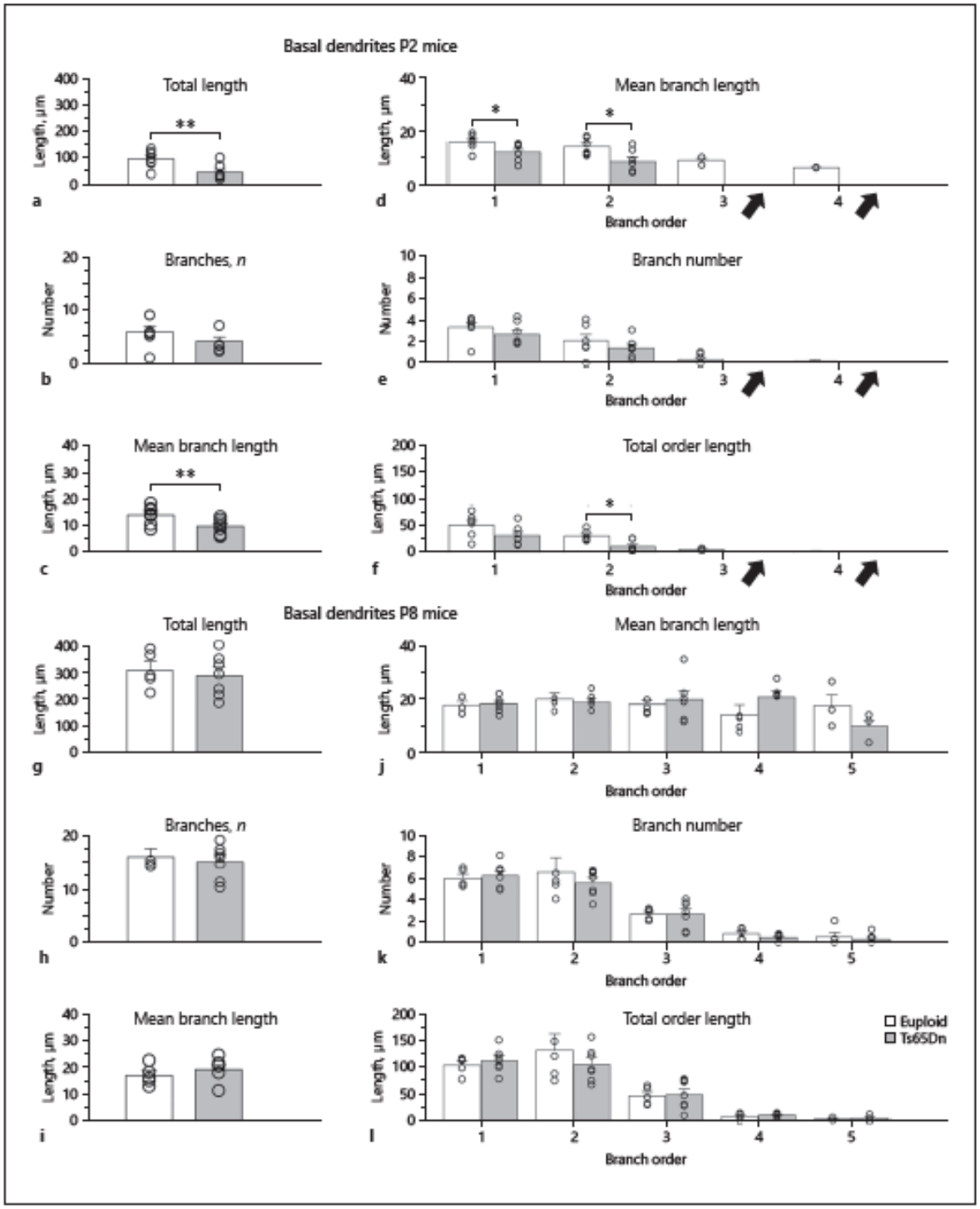

603
604 **Fig. 6**. Morphometry of the basal dendrites of pyramidal neurons in layer II/III of the frontal cortex of P2 and P8
605 euploid and Ts65Dn mice. a–c Quantification of the total length (a), total number of branches (b), and mean branch
606 length (c) in P2 mice. d–f Quantification of the mean length (d), total number (e), and total length (f) of branches of
607 each order in P2 mice. g–i Quantification of the total length (g), total number of branches (h), and mean branch length
608 (i) in P8 mice. j–l Quantification of the mean length (j), total number (k), and total length (l) of branches of each order
609 in P8 mice. Values in (a–l) represent mean ± SE. The scatterplots over each column represent the values of individual
610 cases for each group. The black arrows in (d–f) indicate lack of branches of orders 3 and 4 in P2 Ts65Dn mice. *p <
611 0.05; **p < 0.01; Student's t test or Mann-Whitney U test.
612

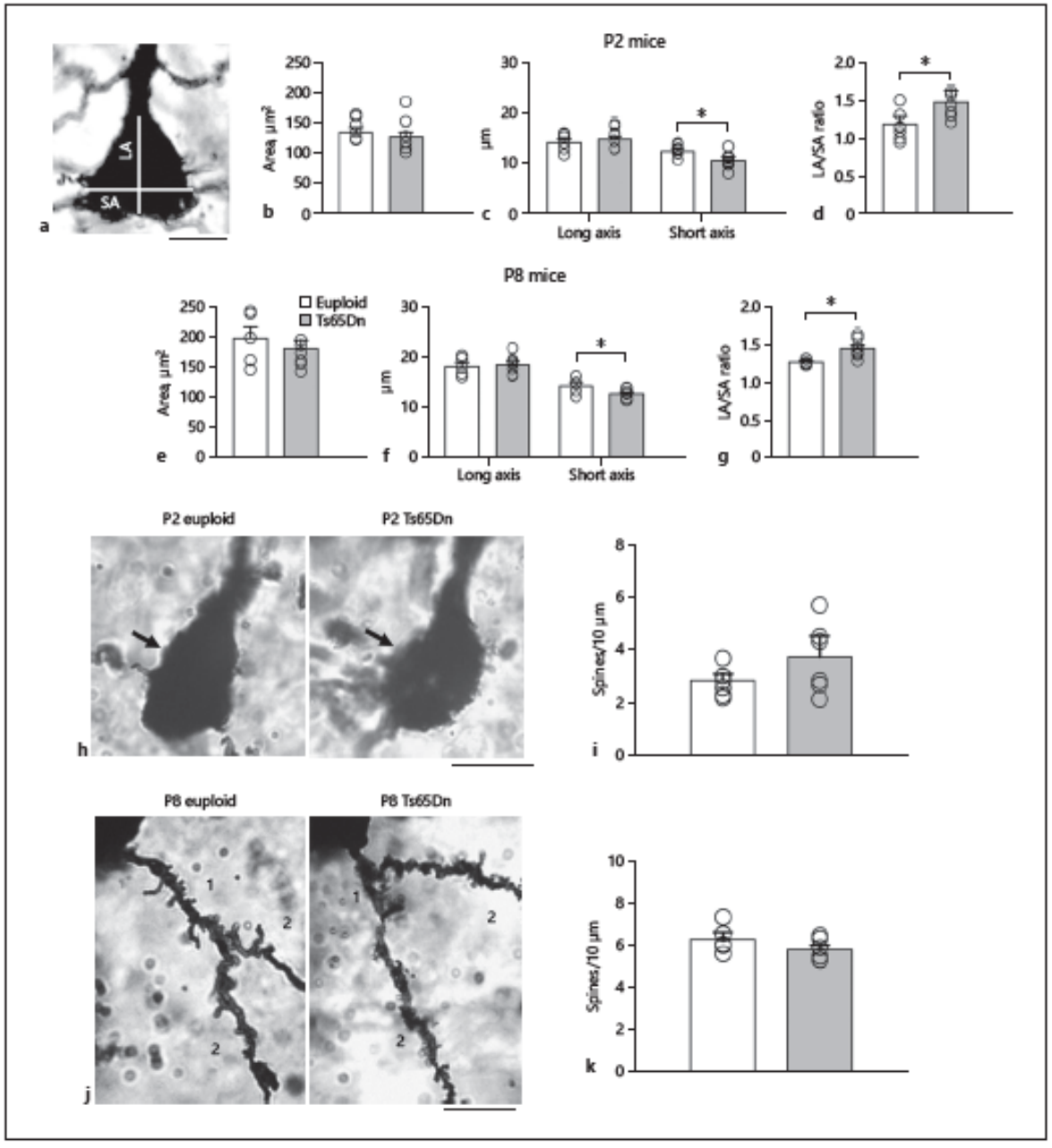

Fig. 7. Parameters of the soma and spine density of pyramidal neurons in layer II/III of the frontal cortex of P2 and P8 euploid and Ts65Dn mice. **b–d** Quantification of the surface area (**b**), LA and SA (**c**), and the ratio between the LA and SA axes (**d**) of layer II/III pyramidal neuron soma in P2 mice. **e**, **f** Quantification of the surface area (**e**), LA and SA (**f**) and ratio between the LA and SA axes of layer II/III pyramidal neuron soma in P8 mice. Axes measurements were taken as shown in (**a**). Calibration bar in (**a**), 10 µm. **h** Images of soma of layer II/III pyramidal neurons in the frontal cortex of an euploid and a Ts65Dn mouse aged 2 days. The arrows point to a somatic spine. Calibration bar, 10 µm. **i** Quantification of spine density on the soma of pyramidal neurons of euploid and Ts65Dn mice aged 2 days. **j** Images of basal dendritic branches of layer II/III pyramidal neurons in the frontal cortex of an euploid and a Ts65Dn mouse aged 8 days. Numbers indicate branches of orders 1 and 2. Calibration bar, 20 µm. **k** Quantification of spine density on the basal dendrites of euploid and Ts65Dn mice aged 8 days. Values in (**b–g**, **i**, **k**) represent mean ± SE. The scatterplots over each column represent the values of individual cases for each group. *$p < 0.05$ Student's *t* test. LA, long axis; SA, short axis.